A larger brown fat volume and lower radiodensity are related to a greater cardiometabolic risk, especially in young men

Short title: Brown adipose tissue and cardiometabolic risk

Authors: Francisco M. Acosta[1,2,3,4], Guillermo Sanchez-Delgado[1,5], Borja Martinez-Tellez[1,6], Francisco J. Osuna-Prieto[1,7,8], Andrea-Mendez Gutierrez[9,10,11], Concepcion M. Aguilera[9,10,11], Angel Gil[9,10,11], Jose M. Llamas-Elvira[12], Jonatan R Ruiz[1].

[1]PROFITH "PRO-moting FITness and Health Through Physical Activity" Research Group, Department of Physical and Sports Education, Sport and Health University Research Institute (iMUDS), Faculty of Sports Science, University of Granada, Granada, Spain.
[2]Turku PET Centre, University of Turku, Turku, Finland.
[3]Turku PET Centre, Turku University Hospital, Turku, Finland.
[4]InFLAMES Research Flagship Center, University of Turku, Finland.
[5]Pennington Biomedical Research Center, Baton Rouge, LA, USA.
[6]Department of Medicine, Division of Endocrinology, and Einthoven Laboratory for Experimental Vascular Medicine, Leiden University Medical Center, Leiden, The Netherlands.
[7]Department of Analytical Chemistry, University of Granada, Granada, Spain.
[8]Research and Development of Functional Food Center (CIDAF), Granada, Spain.
[9]Department of Biochemistry and Molecular Biology II, "José Mataix Verdú" Institute of Nutrition and Food Technology (INYTA), Biomedical Research Centre (CIBM), University of Granada, Granada, Spain.
[10]Biohealth Research Institute in Granada (ibs.GRANADA), Granada, Spain.
[11]CIBER Fisiopatología de la Obesidad y la Nutrición (CIBEROBN), Madrid, Spain.
[12]Nuclear Medicine Services, "Virgen de las Nieves" University Hospital, Granada, Spain.

Corresponding authors:

Francisco M. Acosta, Turku PET Centre, University of Turku, Kiinamyllynkatu 4-8, 20521, Turku, Finland. E-mail fm.acostamanzano@gmail.com

Jonatan Ruiz Ruiz, Department of Physical and Sports Education, Faculty of Sports Science, University of Granada, Carretera de Alfacar s/n, 18071 Granada, Spain. E-mail: ruizj@ugr.es

ClinicalTrial ID (link): NCT02365129 (https://www.clinicaltrials.gov/ct2/show/NCT02365129?term=ACTIBATE&draw=2&rank=1)

Conflicts of interest. None to declare.

Abstract word count: 250

Main text word count: 4000

Number of tables and figures: 5

Number of references: 40

ABBREVIATIONS

ALP: alkaline phosphatase

ALT: alanine aminotransferase

BAT: brown adipose tissue

BMI: body mass index

CMR: cardiometabolic risk

DASH: dietary approaches to stop hypertension

DII: dietary inflammatory index

^{18}F-FDG: ^{18}fluorine-fluordeoxyglucose

GGT: gamma-glutamyl transferase

HDL-C: high-density lipoprotein-cholesterol

HOMA-IR: homeostatic model of assessment of insulin resistance

HOMA-β: homeostatic model assessment of beta-cell function

IFNγ: interferon-gamma

IL: interleukin

LDL-C: low-density lipoprotein-cholesterol

LPL: lipoprotein-lipase

MED: Mediterranean dietary pattern

PET-CT: positron emission tomography-computed tomography

SUV: standardized uptake value

TNFα: tumor necrosis factor alpha

VAT: visceral adipose tissue

ABSTRACT

Brown adipose tissue (BAT) is important in the maintenance of cardiometabolic health in rodents. Whether the same is true in humans is unknown, partly because of the methodological bias that affected previous research. The present work reports the relationships shown by the cold-induced BAT volume, SUV_{peak} (peak standardized uptake) and mean radiodensity (an inverse proxy of the triacylglycerols content) with the cardiometabolic and inflammatory profile of 131 young adults (86 women), and how these relationships are influenced by sex and body weight. All subjects underwent personalized cold exposure for 2 h, followed by static ^{18}F-fluorodeoxyglucose positron emission tomography-computed tomography scanning to determine BAT variables. Information on cardiometabolic risk (CMR) and inflammatory markers was gathered, and a CMR score and fatty liver index (FLI) calculated. In men, BAT volume was found to be positively related to homocysteine and liver damage markers concentrations (independently of BMI and seasonality) and the FLI (all $P \leq 0.05$). In men too, BAT mean radiodensity was negatively related to the glucose and insulin concentrations, alanine aminotransferase activity, insulin resistance, total cholesterol/HDL-C, LDL-C/HDL-C, the CMR score, and the FLI (all $P \leq 0.02$). In women it was only negatively related to the FLI ($P < 0.001$). These associations, however, were driven by the results for the overweight and obese subjects; no such associations were seen in normal-weight subjects. Further, no relationship was seen between BAT and inflammatory markers ($P > 0.05$). These findings suggest that a larger BAT volume and a lower BAT mean radiodensity are related to a higher CMR, especially in young men.

Keywords: brown fat, cardiometabolic risk factors, chronic inflammation, insulin resistance, obesity, thermogenesis.

HIGHLIGHTS

- A greater BAT volume and lower BAT mean radiodensity (indicating a greater triacylglycerol content) are related to increased cardiometabolic risk, especially in young men
- Body weight greatly influences the associations shown by BAT volume and mean radiodensity with the CMR; being these associations only observed in overweight and obese subjects
- BAT volume and mean radiodensity are not related to the inflammatory profile
- These findings call into question the results of retrospective studies performed at thermoneutrality, and provide new insight into the role of BAT in cardiometabolic health

INTRODUCTION

In 2009, it was confirmed that brown adipose tissue (BAT), a thermogenic organ with great potential to prevent obesity and cardiometabolic disease in rodents, was metabolically active in adult humans[1]. Since then, BAT has been shown to dissipate energy as heat mainly via the catabolism of glucose and fatty acids[2,3]. Further, BAT can potentially modulate metabolism body-wide via the secretion of immunometabolic factors[4]. Although the likelihood of human BAT having a role as an anti-obesity agent is low given its scant contribution to daily energy expenditure (10-13 kcal/day when cold-stimulated)[5], it is still to be determined whether it may be beneficial in terms of cardiometabolic risk (CMR) management.

Studies in rodents support the latter idea[2,6,7]. However, in humans the evidence is inconclusive, in part because of the difficulty in designing appropriate experiments, the existence of important confounders, and the lack of mechanistic insight in most earlier work[8–13]. Recently, a retrospective study analyzed BAT volume and activity via ^{18}F-fluorodeoxyglucose positron emission tomography-computed tomography (^{18}F-FDG-PET-CT) in 52,487 patients with cancer[8], and the results suggested it to be associated with improved cardiometabolic health, especially in patients with overweight or obesity. However, as in other previous studies, the ^{18}F-FDG-PET-CT scanning was performed at thermoneutrality, a condition under which functional BAT is likely undetectable. Indeed, to avoid this bias current recommendations state that ^{18}F-FDG–PET-CT scanning should be performed after individualized cold exposure[14]. A clear need exists for data to be collected in new experiments that take all these issues into account.

The present cross-sectional study explores the relationship shown by the cold-induced BAT volume and activity (estimated by ^{18}F-FDG-PET-CT) and BAT mean radiodensity (an indicator of biological tissue density which is inversely related to triacylglycerols

content)[15] with the cardiometabolic and inflammatory profile in a large cohort of relatively healthy, young adults. Special attention was paid to the influence of sex and body weight on these relationships (factors that in previous studies were mostly overlooked), and analyses performed that took into account potential confounders. In addition, BARCIST recommendations were strictly adhered to when analyzing all ^{18}F-FDG-PET-CT-related variables.

MATERIALS AND METHODS

Study subjects and experimental design

This study was performed as part of the ACTIBATE project (ClinicalTrials.gov no. NCT02365129)[16]. Subjects were recruited via advertisements in electronic media and leaflets. The inclusion criteria were: to be 18-25 years old, to be sedentary (self-reported <20 min moderate-vigorous physical activity on <3 days/week), to be a non-smoker, to have had a steady body weight over the last 3 months (change <3 kg), to have no cardiometabolic disease (hypertension, diabetes, etc.), not to be pregnant and not to be regularly exposed to cold environments (e.g., as would be ski monitors or fishmongers). Written, signed, informed consent to be included was obtained from all subjects. All study protocols adhered to the 2013 Declaration of Helsinki and were approved by the Human Research Ethics Committee of the University of Granada (nº 924), and by the Human Research Ethics Committee of the *Junta de Andalucía* (nº 0838-N-2017). All assessments were made in Granada (Spain).

Procedures

All subjects underwent ^{18}F-FDG-PET-CT scanning (to assess BAT variables) over eight dates distributed between October and December of 2015 and 2016, i.e., four dates per year, with one test per subject. The cardiometabolic and inflammatory profiles, anthropometry, body composition and lifestyle behaviours were recorded within three weeks of the ^{18}F-FDG-PET-CT assessment.

^{18}F-FDG-PET-CT scanning

Subjects came to the participating hospital and asked to confirm that they had met the pre-study conditions, i.e.: i) to be arriving in a fasting state (and have been so for at least 6 h), ii) having slept as usual, iii) having refrained from any moderate or vigorous physical activity (within 24 and 48 h respectively), and iv) having not consumed any alcoholic or stimulant (e.g., caffeine) beverages in the previous 6 h. Subjects were then

asked to void their bladder and to dress in standardized clothes (sandals, shorts, and T-shirt), and were directed to a quiet, warm (22-23ºC) room where they seated for 30 min. After this period, subjects were moved into an air-conditioned cold room (19.5-20ºC) where they sat down and were put on a temperature-controlled water-perfused cooling vest (Polar Products Inc., Stow, OH, USA), which covered the clavicular region, the chest, the abdomen and the back. The water temperature of the cooling vest was set 4°C above their individual shivering threshold, which was determined 48-72 h before ^{18}F-FDG-PET-CT scannning[17]. Subjects remained under these conditions for 60 min to induce BAT activation. They were then injected with a bolus of ^{18}F-FDG (183.52±12.21 MBq), with the water temperature of the cooling vest raised by ~1°C for the last 60 min to avoid shivering (or whenever subjects reported shivering). After 2 h, all subjects lay supine in a whole-body PET-CT scanner, and a low dose CT scan (120 kV) was performed for attenuation correction and anatomic localization, followed by static PET consisting of two bed position scans from the atlas vertebra to the mid-chest (6 min each).

The date when the baseline PET-CT scan was performed was recorded as the day of the year (January 1st = day 1, and December 31st = day 365/366; a means of recording the season of the year).

^{18}F-FDG-PET-CT analysis

PET-CT scans were semi-automatically analyzed using the Beth Israel plug-in for FIJI http://sourceforge.net/projects/bifijiplugins/. To determine BAT volume and peak standardized uptake value (SUV_{peak}), six regions of interest (ROIs) were outlined from the atlas vertebra to thoracic vertebra 4 using a 3D-axial technique. These ROIs comprised the supraclavicular, laterocervical, paravertebral and mediastinal regions. To determine BAT mean radiodensity, an ROI covering the scanned body – except the mouth - was outlined from the atlas vertebra to thoracic vertebra 4. Within these ROIs,

the SUV threshold for a voxel to be considered to represent BAT was taken as ≥[1.2 / (lean body mass/body mass)]; the radiodensity also had to fall in the range -190 to -10 Hounsfield units (HU)[14]. The mean BAT volume (average of all ROIs) and SUV_{peak} (i.e., the highest average SUV in a 1-mL spherical volume over all ROIs), and the BAT mean radiodensity were recorded. Subjects were classified as PET+ when they had a BAT volume higher than 7.78 mL (these subjects had a substantial number of BAT voxels within the outlined ROIs) or as PET- if their BAT volume was lower than 7.78 mL. This was determined visually for each PET-CT image. It should be noted that since a whole ROI was drawn to determine BAT mean radiodensity, which included areas where BAT is not typically located, some voxels belonging to connective tissue, internal organs, glands, etc., were erroneously classified as BAT in the PET- subjects (n=31); these subjects were not included in BAT mean radiodensity determinations. A single slice-ROI was also outlined to determine the SUV_{peak} in the subcutaneous white adipose tissue (WAT, used as a reference tissue) next to the triceps brachialis. For the sake of confirmation, BAT SUV_{peak} was recalculated as a product of the percentage lean body mass (SUV_{LBM}).

Cardiometabolic and inflammatory profiles

On a different day, subjects came for the collection of blood samples, at which time they were asked to confirm they met the same requirements as outlined above (See ^{18}F-FDG-PET-CT scanning). Samples were collected in BD Vacutainer® collection tubes, centrifuged, and the serum collected sent to analyze the glycaemic, lipid, hepatic and several inflammatory markers (C-reactive protein, C3, C4, and β-microglobulin 2) concentrations (see below). Plasma samples were aliquoted in smaller volumes and frozen at -80ºC for the later analysis of other inflammatory markers (see below).

Glycaemic, lipid and other markers, and the HOMA index

Serum glucose, total cholesterol, high-density lipoprotein-cholesterol (HDL-C), triacylglycerol and homocysteine concentrations were measured following standard colorimetric methods using an AU5832 automated analyzer (Beckman Coulter Inc., Brea CA, USA). Serum insulin was measured using the Access Ultrasensitive Insulin Chemiluminescent Immunoassay Kit (Beckman Coulter Inc., Brea CA, USA). Low-density lipoprotein-cholesterol (LDL-C) was estimated as: *[total cholesterol – HDL-C – (triacylglycerols/5)]*, in mg/dL[18], and other cardiovascular risk indices, including the total cholesterol/HDL-C and LDL-C/HDL-C ratios, calculated. Insulin resistance was determined via the homeostatic model assessment of insulin resistance (HOMA-IR) using the equation *[insulin (μU/mL) x glucose (mmol/L)]/22.5*, and via the homeostatic model assessment of beta-cell function (HOMA-β) using the equation *[20 x insulin (μU/mL)] / [(glucose (mmol/L) – 3.5]*[19,20].

Systolic, diastolic and mean blood pressure

Systolic and diastolic blood pressure was measured with subjects seated and relaxed, using an Omron M6 upper arm blood pressure monitor (Omron Healthcare Europe B.V. Hoofddorp, The Netherlands). Measurements were taken on three different days, and the mean was determined for use in later analyses. Mean blood pressure was calculated as: *[Systolic blood pressure + (2*Diastolic blood pressure)]/3.*

Cardiometabolic risk score

A CMR score based on variables included in the diagnostic criteria of metabolic syndrome[21] was calculated using a model that includes subject waist circumference, mean blood pressure, glucose, and the HDL-C and triacylglycerol concentrations. Each variable was standardized as follows: standardized value = (value - mean)/standard deviation. The HDL-C standardized values were multiplied by -1 in keeping with the negative scores for the other CMRs. The final score was determined as the average of

the five standardized scores. The final CMR score was calculated separately for men and women.

Hepatic enzymes and fatty liver index

The serum alanine aminotransferase (ALT), gamma-glutamyl transferase (GGT) and alkaline phosphatase (ALP) activities were determined by standard colorimetric methods, using an AU5832 automated analyzer (Beckman Coulter Inc., Brea, CA, USA). The FLI (FLI) was calculated using a simple but accurate predictor of hepatic steatosis in the general population[22], i.e., $=(e^{0.953*\log e(\text{triacylglycerols}) + 0.139*BMI + 0.718*\log e(GGT) + 0.053*\text{waist circumference} - 15.745}) / (1 + e^{0.953*\log e(\text{triacylglycerols}) + 0.139*BMI + 0.718*\log e(GGT) + 0.053*\text{waist circumference} - 15.745}) * 100$. As previously reported[22], a FLI of <30 was used to rule out hepatic steatosis, whereas a value of >60 was used to indicate its presence[22].

Inflammatory markers

Serum C-reactive protein, C3, C4, and β-microglobulin 2 concentrations were measured by immunoturbidimetric assay, employing the same AU5832 automated analyzer as above. Plasma interleukin (IL)-2, IL-4, IL-6, IL-7, IL-8, IL-10, IL-17a, interferon gamma (IFNγ) and tumor necrosis factor alpha (TNFα) were determined using the MILLIPLEX MAP Human High Sensitivity Cytokine Panel (Luminex Corp., Clayton, MO, USA). Leptin and adiponectin concentrations were measured using Panels 1 and 2 (respectively) of the MILLIPLEX MAG/MAP Human Adipokine Magnetic Bead Kits (Luminex Corp.).

Anthropometry, body composition and lifestyle behaviours

Subject weight and height were measured using a model 799 SECA scale and stadiometer (Electronic Column Scale, Hamburg, Germany). BMI was calculated as *body weight (kg)/height in* m^2, and used to classify subjects as normal weight (BMI ≥18 and <25 kg/m^2), overweight (BMI ≥25 and <30 kg/m^2) or obese (BMI ≥30 kg/m^2). Waist circumference was measured at the minimum perimeter, or when subjects showed

abdominal obesity in a horizontal plane above the umbilicus. Fat mass, lean mass and visceral adipose tissue (VAT) mass were determined by dual-energy x-ray absorptiometry using a Discovery Wi device (Hologic, Bedford, Massachusetts, USA). The fat mass index was calculated as *fat mass/heigh in* m^2.

Sedentary time, overall physical activity and sleep duration were objectively measured by accelerometry over 7 consecutive days[17,23]. Subjects' daily energy intake was estimated via an *ad libitum* meal test[24]. Moreover, self-reported daily energy and macronutrient intake, and adherence to different dietary patterns (i.e., Mediterranean Dietary Patter [MED], Dietary Approach to Stop Hypertension [DASH], and Dietary Inflammatory Index [DII]), were assessed using data obtained from three non-consecutive 24 h dietary recalls and a food frequency questionnaire. More details are provided in **Appendix A**.

Statistical analyses

Table 1 show the descriptive statistics for the study subjects. Continuous variables are presented as means (standard deviation) when normally distributed or medians (interquartile range) when not. Categorical variables are presented as numbers (percentage). The effect of the interaction between BAT variables and sex on the cardiometabolic and inflammatory profiles was examined by linear regression. Since an interaction effect was observed for several outcomes, all analyses were performed separately for men and women. Several extreme cases, confirmed as influential outliers with respect to the outcome variables, were corrected using a subtle version of winsorizing (**Appendix B**). In some cases, optimum Box-Cox transformations were employed to normalize data.

Potential confounders (i.e., according to prior evidence[23,25–27]) or that were statistically related to predictors/outcomes, were included in the models used in the primary and sensitivity analyses. Multiple linear regression was used to analyse the relationship

shown by BAT volume, SUV_{peak} and mean radiodensity with the cardiometabolic and the inflammatory profiles (**Tables 2** and **3**, respectively). Adjustments were then made for BMI, and for BMI plus the PET-CT scan date. The associations between BAT variables and the FLI were not adjusted for BMI in any model since this was one of the components included in the algorithm to calculate the FLI. Additional analyses were performed to determine whether the relationships shown by the BAT variables with the cardiometabolic and inflammatory profiles were dependent in body weight (**Figure 2**). Body weight was classified as normal-weight, overweight or obese in analyses related to BAT volume and SUV_{peak}, and as normal-weight and overweight-obese in analyses related to BAT mean radiodensity (a reduced number of obese subjects were available for this analysis). Adjustments for multiple comparison errors (familywise error rate [Hochberg procedure]) were made for the main analyses (**Tables 2 and 3**).

Analyses were performed using SPSS-26.0 software (IBM, NY, USA), Significance was set at $P \leq 0.05$ for the linear correlation and regression analyses, and at $P < 0.1$ for the effects of interactions.

RESULTS

A total of 131 subjects (86 women) were included in this study (see Flow Chart, **Figure S1**). **Table 1** shows the main characteristics of the study subjects.

A larger BAT volume and lower BAT mean radiodensity are related to increased cardiometabolic risk, especially in young men

In men, but not women, BAT volume was positively associated with the homocysteine, GGT and ALP activities, and the FLI (all P≤0.02, **Table 2**). In men too, BAT mean radiodensity was positively related to the HDL-C concentrations, and inversely related to the glucose and insulin concentrations, HOMA-IR, HOMA-B, TC/HDL-C and LDL-C/HDL-C, to the CMR score, and the FLI (all P≤0.02).

In women, BAT mean radiodensity was negatively related to the ALP activity and the FLI (all P≤0.03). **Figure 1** shows the scatter plots for the associations between the BAT variables and the CMR score and FLI, both in terms of subject sex and body weight.

When all these analyses were repeated adjusting for BMI, or for the BMI and PET-CT scan date (data not shown), the association between BAT volume and the HDL-C concentration became significant (P=0.01), and the associations between BAT mean radiodensity and the CMR markers became non-significant (all P>0.05) - except for the HDL-C concentration in men. After adjusting for multiplicity, all associations were non-significant in women (all P>0.05), as were the associations between BAT mean radiodensity and most of the CMR markers in men, although its associations with the insulin levels, HOMA-IR, CMR score, and the FLI, remained significant (all P≤0.01).

BAT variables are not related to inflammatory markers

In men, BAT volume and SUV_{peak} were positively related to the C3 concentration; BAT mean radiodensity was negatively related to the C3 concentration, and positively to the adiponectin concentrations (all P≤0.03, **Table 3**). In women, BAT volume was positively associated with the C-reactive protein concentration, whereas BAT mean

radiodensity was negatively related to it and the C3 concentration, but positively related to the IL-10 concentration. When these analyses were adjusted for BMI, or for BMI and the PET-CT scan date, the associations between BAT mean radiodensity and adiponectin (in men) and C3 (in women) became non-significant ($P>0.05$, data not shown). After adjusting for multiplicity, all associations became non-significant ($P>0.05$).

Body weight influenced the relationship shown by BAT variables with cardiometabolic risk and inflammatory markers

The relationship shown by the BAT variables with the CMR and inflammatory markers were also examined in men and women according to their body weight (see **Figure 2**); BMI has previously been reported to influence these variables[27] (see **Table S1**).

In men, BAT volume was positively related to the total cholesterol, LDL-C, and homocysteine concentrations in the overweight group ($r=0.56$-0.65, all $P<0.06$), and to the HDL-C ($r=0.7$, $P=0.008$) in the obesity group. Further, in men with obesity, BAT mean radiodensity was inversely related to the glucose and insulin concentrations, and the HOMA-IR and HOMA-B scores ($r=-0.61$ to -0.75, all $P<0.09$), and positively related to HDL-C ($r=0.54$, $P\leq0.09$). However, none of these associations was observed in women (all $P>0.05$). Similarly heterogeneous patterns were observed for the associations between BAT variables and inflammatory markers. **Figures S2 and S3** show the scatter plots for all the significant relationships detected. It should be noted that the PET-CT scan date was similar across all groups (all $P>0.05$, see **Figure S4**).

Sensitivity analyses important for the interpretation of the current results are provided in the **Appendix C.**

DISCUSSION

This study examines the relationships shown by BAT volume, SUV_{peak} and mean radiodensity with the CMR and inflammatory markers for the largest cohort of young adults in which BAT ^{18}F-FDG uptake has been assessed following individualized cold exposure, and strictly adhering to current methodological recommendations. The young age of the subjects likely prevents the ^{18}F-FDG results from being biased by age-induced insulin resistance or BAT dysfunction. In contrast to that reported in previous studies, the present findings suggest that a higher BAT volume and a lower BAT mean radiodensity are associated with increased CMR, especially in young men. Body weight greatly influenced all the associations shown by BAT volume and mean radiodensity with the CMR markers – being these associations driven by the results for the overweight and obese subjects. BAT variables were not related to inflammatory marker concentrations. These findings call into question the results reported in previous retrospective studies performed at thermoneutrality, and provide new insight into the role of BAT in cardiometabolic health.

Recent studies in adult humans have suggested that a larger BAT volume/prevalence (assessed by static ^{18}F-FDG-PET-CT) or a lower supraclavicular fat fraction (assessed by magnetic resonance imaging, MRI), either in warm[8,13] or cold conditions[10,28], are related to better cardiometabolic health. In contrast, the present results suggest that a larger BAT volume is related to an increase in several markers of CMR, especially in men. The lack of prior evidence regarding how BAT volume relates to CMR in men and women precludes any comparison. However, it is well known that men preferentially accumulate fat in the upper body adipose depots (e.g., VAT), whereas premenopausal women accumulate fat mainly in the gluteofemoral depots; this prompts the regularly observed higher CMR in men[29]. It might therefore be speculated that in men with elevated CMR markers, BAT could be recruited to help maintain metabolic

homeostasis. This hypothesis is in line with the classic studies of Rothwell et al. (1997)[30], showing that obesity induced in mice by cafeteria or high-fat diets is accompanied by an increase in BAT mass. Accordingly, men with a higher overall and central adiposity have a larger cold-induced BAT volume[27], and young men with obesity have a larger BAT volume compared to their normal-weight peers (in the present work, 85% were PET+, see **Figure S5**).

The discrepancies between the present and previous studies[10–13] cannot be explained by a single factor. For example, in a cohort likes ours, the low prevalence of insulin resistance – which is related to impaired BAT ^{18}F-FDG uptake[31] - , is less likely to bias the ^{18}F-FDG related measures than when examining older or diseased populations. In addition, most previous studies have involved a small sample size, preventing confounders (e.g., environmental temperature, age, lifestyle behaviours) or the influence of sex being taken into account. In addition, the methodological approach has varied greatly across studies. For instance, few studies exposed subjects to cooling before performing a BAT ^{18}F-FDG-PET-CT scan, an oversight likely to render a large proportion of the functional BAT undetectable, biasing the results. Moreover, many studies did not follow the international BARCIST recommendations for measuring and analysing BAT ^{18}F-FDG variables[32].

Should future studies show that BAT recruitment is important for metabolic homeostasis in humans, the underlying mechanisms will need to be investigated. It has been argued that BAT may contribute directly to the prevention of obesity and the reduction of CMR by increasing daily energy expenditure and systemic glucose and non-esterifed fatty acid (NEFA) turnover – although so far the indications are that this is unlikely[3,5,33]. However, rodent experiments show that BAT may also act through indirect mechanisms, or via the release of different immunometabolic factors,

modulating whole-body metabolism[4,6,7]. For instance, when exposed to cold, murine BAT generates small HDL particles, accelerating HDL turnover and reducing cholesterol transport to the liver[34]. Paradoxically, in the present work, subjects with a larger BAT volume had higher levels of HDL-C (when adjusted for BMI or BMI plus the PET-CT scan date), even though BAT volume was positively related to CMR markers. Future studies are needed to ascertain the significance of this finding, but it may support an indirect role for BAT in the regulation of human metabolism (conserved even in states of metabolic disruption). Certainly, it has been shown that brown fat-secreted factor neuregulin 4 (Nrg4) preserves metabolic homeostasis via the attenuation of hepatic lipogenesis[35], and positive associations between BAT volume with activities of hepatic enzymes, and with the FLI (a proxy of hepatic steatosis[22]), are shown in the present work. This may support the importance of a BAT-liver axis for maintaining metabolic homeostasis.

The present findings also show that men with a higher CMR had a lower BAT mean radiodensity. Indeed, systemic markers/scores of insulin resistance, insulin secretion dysfunction, dyslipidemia and hepatic dysfunction were related to lower BAT mean radiodensity in men, and those men with metabolic syndrome had a lower BAT mean radiodensity (**Figure S6**). Accordingly, we recently reported that overall and central adiposity were moderately related to lower BAT mean radiodensity in men, and weakly related to this in women[27]. It is known that in obesity, lipids tend to accumulate in ectopic depots, promoting lipotoxic effects such as insulin resistance or inflammation, which lead to tissue dysfunction[36] – and this may also be the case with human BAT. Indeed, BAT glucose and NEFA uptake and perfusion are reduced in subjects with obesity compared to their lean counterparts in warm and cold conditions[37,38]. In addition, the correlation between BAT mean radiodensity and the FLI may indicate that

ectopic lipid accumulation in both tissues occurs (in parallel) in obesity or states of metabolic disruption.

A recent study[8] reported that PET+ subjects (i.e., with detectable BAT) had better cardiometabolic health than those who were PET-, with more pronounced effects in patients with overweight or obesity. It is noteworthy, however, that ^{18}F-FDG PET-CT scans were performed in warm conditions, and most subjects were qualitatively classified as having BAT or not. In addition, that work contained many old and/or diseased persons, some of whom were insulin resistant (i.e., had impaired BAT ^{18}F-FDG uptake[31]), which limited the conclusions that could be drawn on the moderating role of body weight on the relationships observed. The present work, however, reveals that associations shown by BAT volume and BAT mean radiodensity with CMR markers occur in men with overweight/obesity. This suggests that the contribution of the BAT to metabolic regulation might be more significant in states of metabolic disruption, such as obesity.

Limitations of the study

The present results should be interpreted with caution; the cross-sectional study design precludes the establishment of causal relationships. Further, the sample was composed of young, relatively healthy men and women; this could have masked or weakened the associations of the BAT variables with the CMR and inflammatory profiles. Although the use of the shivering threshold as the end-point of the personalized cold exposure is widely used in the field, it could have affected the thermal stress to which each subject was submitted, introducing differences in BAT variables results[39]. BAT ^{18}F-FDG uptake was quantified using the most commonly employed technique and following current recommendations[14]. However, static ^{18}F-FDG-PET-CT scans suffer several limitations that may prevent a fully accurate estimation of cold-induced BAT metabolic

activity[40]. Finally, the multiplicity and sensitivity analyses should be considered when interpreting the present results.

In conclusion, the present results suggest that a larger BAT volume and a lower BAT mean radiodensity are associated with an increased CMR, especially in young men. Body weight greatly influences the associations between BAT variables and CMR - associations observed only in the overweight and obese groups. BAT variables were not related to inflammatory markers. Future studies should investigate whether these findings are replicated in other populations, and in longitudinal studies, and determine the underlying mechanisms linking BAT and cardiometabolic health.

ACKNOWLEDGMENTS

Authors' contributions. FAM, GSD, BMT, CMA, AG, JMLLE and JRR designed the study; FAM, GSD, BMT and AMG conducted the experiments; CMA, AG, JMLLE and JRR provided essential reagents and materials; FAM, GSD, BMT, FJOP and AMG analyzed the data and performed the statistical analysis; FAM wrote the manuscript; FAM, GSD, BMT, FJOP, AMG, CMA, AG, JMLLE and JRR reviewed the manuscript and provided scientific assistance; JRR had primary responsibility for the paper's final content.

Funding: This study was funded by the Spanish Ministry of Economy and Competitiveness via the *Fondo de Investigación Sanitaria del Instituto de Salud Carlos III* (PI13/01393) and PTA 12264-I, by *Retos de la Sociedad* (DEP2016-79512-R), European Regional Development Funds (ERDF), the Spanish Ministry of Education (FPU 13/03410, FPU16/02828, FPU16/03653), the *Fundación Iberoamericana de Nutrición* (FINUT), the *Redes Temáticas de Investigación Cooperativa* RETIC network (Red SAMID RD16/0022), the AstraZeneca HealthCare Foundation, the University of Granada's *Plan Propio de Investigación 2016* - Excellence actions: Unit of Excellence on Exercise and Health (UCEES), the *Junta de Andalucía*, *Consejería de Conocimiento, Investigación y Universidades* (ERDF, SOMM17/6107/UGR), the *Fundación Alfonso Martin Escudero*, and the *InFLAMES Flagship Programme* of the Academy of Finland (decision number: 337530).

REFERENCES

1. Virtanen KA, Lidell ME, Orava J, et al. Functional brown adipose tissue in healthy adults. *N Engl J Med*. 2009;360(15):1518-1525. doi:10.1056/NEJMoa0808949

2. Ruiz JR, Martinez-Tellez B, Sanchez-Delgado G, Osuna-Prieto FJ, Rensen PCN, Boon MR. Role of Human Brown Fat in Obesity, Metabolism and Cardiovascular Disease: Strategies to Turn Up the Heat. *Prog Cardiovasc Dis*. 2018;61(2):232-245. doi:10.1016/j.pcad.2018.07.002

3. Carpentier AC, Blondin DP, Virtanen KA, Richard D, Haman F, Turcotte ÉE. Brown Adipose Tissue Energy Metabolism in Humans. 2018;9(August):1-21. doi:10.3389/fendo.2018.00447

4. Villarroya F, Cereijo R, Villarroya J, Giralt M. Brown adipose tissue as a secretory organ. *Nat Rev Endocrinol*. 2017;13(1):26-35. doi:10.1038/nrendo.2016.136

5. u Din M, Raiko J, Saari T, et al. Human brown adipose tissue [15O]O2 PET imaging in the presence and absence of cold stimulus. *Eur J Nucl Med Mol Imaging*. 2016;43(10):1878-1886. doi:10.1007/s00259-016-3364-y

6. Stanford KI, Middelbeek RJW, Townsend KL, et al. Brown adipose tissue regulates glucose homeostasis and insulin sensitivity. *J Clin Invest*. 2013;123(1):215-223. doi:10.1172/JCI62308

7. Bartelt A, Bruns OT, Reimer R, et al. Brown adipose tissue activity controls triglyceride clearance. *Nat Med*. 2011;17(2):200-206. doi:10.1038/nm.2297

8. Becher T, Palanisamy S, Kramer DJ, et al. Brown adipose tissue is associated with cardiometabolic health. *Nat Med*. 2021;27(1):58-65. doi:10.1038/s41591-020-1126-7

9. Wibmer AG, Becher T, Eljalby M, et al. Brown adipose tissue is associated with healthier body fat distribution and metabolic benefits independent of regional adiposity. *Cell Reports Med*. 2021;2(7):100332. doi:10.1016/j.xcrm.2021.100332

10. Sun L, Yan J, Goh HJ, et al. Fibroblast Growth Factor-21, Leptin, and Adiponectin Responses to Acute Cold-Induced Brown Adipose Tissue Activation. *J Clin Endocrinol Metab*. 2020;105(3):e520-e531. doi:10.1210/clinem/dgaa005

11. Mihalopoulos NL, Yap JT, Beardmore B, Holubkov R, Nanjee MN, Hoffman JM. Cold-Activated Brown Adipose Tissue is Associated with Less Cardiometabolic Dysfunction in Young Adults with Obesity. *Obesity*. 2020;28(5):916-923. doi:10.1002/oby.22767

12. Herz CT, Kulterer OC, Prager M, et al. Active Brown Adipose Tissue is Associated With a Healthier Metabolic Phenotype in Obesity. *Diabetes*. Published online October 18, 2021:db210475. doi:10.2337/db21-0475

13. Franssens BT, Hoogduin H, Leiner T, van der Graaf Y, Visseren FLJ. Relation between brown adipose tissue and measures of obesity and metabolic dysfunction

in patients with cardiovascular disease. *J Magn Reson Imaging*. 2017;46(2):497-504. doi:10.1002/jmri.25594

14. Chen KY, Cypess AM, Laughlin MR, et al. Brown Adipose Reporting Criteria in Imaging STudies (BARCIST 1.0): Recommendations for Standardized FDG-PET/CT Experiments in Humans. *Cell Metab*. 2016;24(2):210-222. doi:10.1016/j.cmet.2016.07.014

15. Din MU, Raiko J, Saari T, et al. Human brown fat radiodensity indicates underlying tissue composition and systemic metabolic health. *J Clin Endocrinol Metab*. 2017;102(7):2258-2267. doi:10.1210/jc.2016-2698

16. Sanchez-Delgado G, Martinez-Tellez B, Olza J, et al. Activating brown adipose tissue through exercise (ACTIBATE) in young adults: Rationale, design and methodology. *Contemp Clin Trials*. 2015;45:416-425. doi:10.1016/j.cct.2015.11.004

17. Acosta FM, Sanchez-Delgado G, Martinez-Tellez B, et al. Sleep duration and quality are not associated with brown adipose tissue volume or activity-as determined by 18F-FDG uptake, in young, sedentary adults. *Sleep*. 2019;42(12). doi:10.1093/sleep/zsz177

18. Friedewald WT, Levy RI, Fredrickson DS. *Estimationof the Concentration of Low-Density LipoproteinCholesterol in Plasma,Without Useof the PreparativeUltracentrifuge*. Vol 18.; 1972. Accessed February 14, 2019. http://clinchem.aaccjnls.org/content/clinchem/18/6/499.full.pdf

19. Matthews DR, Hosker JR, Rudenski AS, Naylor BA, Treacher DF, Turner RC. *Homeostasis Model Assessment: Insulin Resistance and Fl-Cell Function from Fasting Plasma Glucose and Insulin Concentrations in Man*. Vol 28.; 1985. Accessed August 20, 2018. https://link.springer.com/content/pdf/10.1007/BF00280883.pdf

20. Wallace TM, Levy JC, Matthews DR. Use and abuse of HOMA modeling. *Diabetes Care*. 2004;27(6):1487-1495. doi:10.2337/diacare.27.6.1487

21. Alberti KGMM, Eckel RH, Grundy SM, et al. Harmonizing the metabolic syndrome: A joint interim statement of the international diabetes federation task force on epidemiology and prevention; National heart, lung, and blood institute; American heart association; World heart federation; International . *Circulation*. 2009;120(16):1640-1645. doi:10.1161/CIRCULATIONAHA.109.192644

22. Bedogni G, Bellentani S, Miglioli L, et al. The fatty liver index: A simple and accurate predictor of hepatic steatosis in the general population. *BMC Gastroenterol*. 2006;6(1):1-7. doi:10.1186/1471-230X-6-33

23. Acosta FM, Martinez-Tellez B, Sanchez-Delgado G, et al. Association of Objectively Measured Physical Activity with Brown Adipose Tissue Volume and Activity in Young Adults. *J Clin Endocrinol Metab*. 2018;104(2):223-233. doi:10.1210/jc.2018-01312

24. Sanchez-Delgado G, Acosta FM, Martinez-Tellez B, et al. Brown adipose tissue volume and 18F-fluorodeoxyglucose uptake are not associated with energy intake in young human adults. *Am J Clin Nutr*. 2020;111(2):329-339. doi:10.1093/ajcn/nqz300

25. Jurado-Fasoli L, Merchan-Ramirez E, Martinez-Tellez B, et al. Association between dietary factors and brown adipose tissue volume/18F-FDG uptake in young adults. *Clin Nutr*. 2021;40(4):1997-2008. doi:10.1016/j.clnu.2020.09.020

26. Sanchez-Delgado G, Acosta FM, Martinez-Tellez B, et al. Brown adipose tissue volume and 18F-fluorodeoxyglucose uptake are not associated with energy intake in young human adults. *Am J Clin Nutr*. 2020;111(2):329-339. doi:10.1093/ajcn/nqz300

27. Sanchez-Delgado G, Martinez-Tellez B, Acosta FM, et al. Brown Adipose Tissue Volume and Fat Content are Positively Associated with Whole-Body Adiposity in Young Men, Not in Women. *Diabetes*. Published online April 15, 2021:db210011. doi:10.2337/db21-0011

28. Ahmed BA, Ong FJ, Barra NG, et al. Lower brown adipose tissue activity is associated with non-alcoholic fatty liver disease but not changes in the gut microbiota. *Cell Reports Med*. 2021;2(9):100397. doi:10.1016/j.xcrm.2021.100397

29. Karpe F, Pinnick KE. Biology of upper-body and lower-body adipose tissue - Link to whole-body phenotypes. *Nat Rev Endocrinol*. 2015;11(2):90-100. doi:10.1038/nrendo.2014.185

30. Rothwell NJ. A role for brown adipose tissue in diet-induced thermogenesis. *Obes Res*. 1997;5(6):650-656. doi:10.1002/j.1550-8528.1997.tb00591.x

31. Blondin DP, Labbé SM, Noll C, et al. Selective impairment of glucose but not fatty acid or oxidative metabolism in brown adipose tissue of subjects with type 2 diabetes. *Diabetes*. 2015;64(7):2388-2397. doi:10.2337/db14-1651

32. Chen KY, Cypess AM, Laughlin MR, et al. Brown Adipose Reporting Criteria in Imaging STudies (BARCIST 1.0): Recommendations for Standardized FDG-PET/CT Experiments in Humans. *Cell Metab*. 2016;24(2):210-222. doi:10.1016/j.cmet.2016.07.014

33. Muzik O, Mangner TJ, Leonard WR, Kumar A, Janisse J, Granneman JG. 15O PET Measurement of Blood Flow and Oxygen Consumption in Cold-Activated Human Brown Fat. *J Nucl Med*. 2013;54(4):523-531. doi:10.2967/jnumed.112.111336

34. Bartelt A, John C, Schaltenberg N, et al. Thermogenic adipocytes promote HDL turnover and reverse cholesterol transport. *Nat Commun*. 2017;8(1):1-10. doi:10.1038/ncomms15010

35. Wang GX, Zhao XY, Meng ZX, et al. The brown fat-enriched secreted factor Nrg4 preserves metabolic homeostasis through attenuation of hepatic lipogenesis. *Nat Med*. 2014;20(12):1436-1443. doi:10.1038/nm.3713

36. Virtue S, Vidal-Puig A. Adipose tissue expandability, lipotoxicity and the Metabolic Syndrome - An allostatic perspective. *Biochim Biophys Acta - Mol Cell Biol Lipids*. 2010;1801(3):338-349. doi:10.1016/j.bbalip.2009.12.006

37. Din MU, Raiko J, Saari T, et al. Human brown fat radiodensity indicates underlying tissue composition and systemic metabolic health. *J Clin Endocrinol Metab*. 2017;102(7):2258-2267. doi:10.1210/jc.2016-2698

38. Saari TJ, Raiko J, U-Din M, et al. Basal and cold-induced fatty acid uptake of

human brown adipose tissue is impaired in obesity. *Sci Rep*. 2020;10(1):14373. doi:10.1038/s41598-020-71197-2

39. Acosta FM, Martinez-Tellez B, Sanchez-Delgado G, et al. Physiological responses to acute cold exposure in young lean men. *PLoS One*. 2018;13(5). doi:10.1371/journal.pone.0196543

40. Schilperoort M, Hoeke G, Kooijman S, Rensen PCN. Relevance of lipid metabolism for brown fat visualization and quantification. *Curr Opin Lipidol*. 2016;27(3):242-248. doi:10.1097/MOL.0000000000000296

	ALL (n=131)			MEN (n=45)			WOMEN (n=86)			P-value
Age (years)	131	22	(20, 24)	45	22	(20, 24)	86	22	(2)	0.25
Professional status, n (%)										0.18
Student	65		(53.1)	22		(51.2)	43		(50.6)	
Unemployed	48		(37.5)	13		(30.2)	35		(41.2)	
Other professional activities	15		(11.7)	8		(18.6)	7		(8.2)	
Anthropometry and body composition										
Weight (kg)	131	67.9	(58.9, 80.2)	45	79.4	(71.6, 97.1)	86	64.4	(12.2)	**<0.001**
Height (cm)	131	168.5	(8.7)	45	176.1	(6.6)	86	164.5	(6.8)	**<0.001**
BMI (kg/m^2)	131	23.9	(21.6, 27.6)	45	25.8	(23.1, 31.9)	86	23.1	(20.5, 26.7)	**<0.001**
Waist circumference (cm)	129	79.5	(70, 89.1)	45	91.0	(15.7)	84	76.0	(11)	**<0.001**
Weight status, n (%)										**0.006**
Normal-weight	79		(60.3)	20		(44.4)	59		(68.6)	
Overweight	31		(23.7)	12		(26.7)	19		(22.1)	
Obese	21		(16)	13		(28.9)	8		(9.3)	
LMI (kg/m^2)	131	14.7	(2.5)	45	17.3	(2.1)	86	13.4	(1.4)	**<0.001**
FMI (kg/m^2)	131	8.2	(6.3, 11)	45	7.3	(5.9, 11.3)	86	8.9	(6.5, 11)	0.24
Body fat (%)	131	36.3	(30.1, 41.4)	45	29.9	(25.2, 37)	86	38.8	(32.2, 42.7)	**<0.001**
VAT mass (g)	131	312	(197, 457)	45	392	(286, 570)	86	265	(161, 368)	**<0.001**
PET-CT parameters										
Individualized SUV threshold	131	2.1	(0.2)	45	1.9	(1.7, 2.1)	86	2.1	(1.9, 2.3)	**<0.001**
BAT volume (mL)	131	65.1	(12.5, 110)	45	74.6	(8.2, 146)	86	57.5	(11.8, 105.3)	0.22
BAT SUV_{peak}	131	10.8	(4.1, 16.8)	45	9.8	(3, 16)	86	11.5	(4.3, 17.3)	0.29
BAT mean radiodensity (HU)	97	-60.6	(94)	31	-60.9	(8.7)	66	-60.4	(9.8)	0.79
Number of PET+ subjects (%)	100		(76.3)	34		(75.5)	66		(76.7)	0.52
WAT SUV_{peak}	111	0.14	(0.11, 0.19)	38	0.15	(0.11, 0.21)	73	0.15	(0.06)	0.14
Cardiometabolic Profile										
Glucose (mg/dL)	131	87	(83, 92)	45	89.4	(8.1)	86	87.1	(5.8)	0.1
Insulin (uIU/mL)	131	6.9	(5.1, 10.5)	45	6.9	(5, 11.3)	86	7	(5.2, 9.7)	0.84
HOMA-IR	131	1.5	(1.1, 2.2)	45	1.4	(1, 2.5)	86	1.5	(1.1, 2.1)	0.76
HOMA-β	131	113	(78.7, 154.8)	45	102.4	(73.1, 157.7)	86	120	(45.8)	0.8
Total cholesterol (mg/dL)	131	158	(143, 177)	45	153	(142, 176)	86	161	(142, 183)	0.44
LDL-C (mg/dL)	131	95.4	(25.9)	45	91	(82.5, 108)	86	92	(74.8, 107.3)	0.38
HDL-C (mg/dL)	131	51	(47, 59)	45	46.1	(7.8)	86	53	(49, 63)	**<0.001**
Total cholesterol/HDL-C	131	3	(2.6, 3.6)	45	3.4	(2.9, 4)	86	2.9	(2.6, 3.3)	**<0.001**
LDL-C/HDL-C	131	1.7	(1.4, 2.3)	45	2.1	(1.7, 2.6)	86	1.7	(1.4, 2)	**<0.001**
Triacylglycerols (mg/dL)	131	70	(52, 100)	45	76	(57, 108.5)	86	68.5	(52, 89.5)	0.24
Homocysteine (µmol/L)	131	10.2	(8.7, 12.2)	45	11.8	(9.9, 15.4)	86	9.4	(8.3, 10.9)	**<0.001**
Systolic blood pressure (mmHg)	129	117	(12)	44	125	(117, 136)	85	111.9	(9.2)	**<0.001**
Diastolic blood pressure (mmHg)	129	71	(67, 75)	44	73	(67, 78)	85	70.0	(6.3)	**0.05**
Mean blood pressure (mmHg)	129	86.1	(7.9)	44	90.3	(8.6)	85	83.9	(6.6)	**<0.001**
Cardiometabolic risk score	127	-0.1	(-0.4, 0.2)	44	0.1	(-0.1, 0.8)	83	-0.2	(0.5)	**<0.001**
Metabolic syndrome prevalence (%, ATP III)	7		(5.3)	7		(15.6)	0		(0)	
Hepatic Function										
ALT (U/L)	130	14	(12, 20)	45	20	(15, 31)	85	12	(11, 15)	**<0.001**
GGT (U/L)	130	14	(11.8, 20)	45	22	(16, 32.5)	85	13	(11, 15)	**<0.001**
ALP (U/L)	131	71	(59, 84)	45	77	(64.5, 89)	86	68.9	(17.5)	**0.004**
FLI	127	8.88	(4.24, 24.7)	44	25	(10.1, 61.7)	83	6.9	(3.1, 15.7)	**<0.001**
<30 (rule out hepatic steatosis)	100		(76.3)	24		(53.3)	76		(88.4)	
≥60 (rule in hepatic steatosis)	16		(12.2)	13		(28.9)	3		(3.5)	
Inflammatory Profile										
C-reactive protein (mg/L)	131	1.2	(0.7, 2.7)	45	1.2	(0.8, 3.2)	86	1.2	(0.7, 2.5)	0.82
IL-2 (pg/mL)	109	2.3	(1.4)	39	19	(1.4)	70	2.3	(1.6, 3.4)	**0.01**
IL-4 (pg/mL)	109	10.2	(5.8, 16.1)	39	8	(4, 12.8)	70	10.8	(7, 16.4)	0.08
IL-6 (pg/mL)	109	1.1	(0.5, 2.4)	39	0.7	(0.4, 2.1)	70	1.2	(0.6, 2.5)	0.21
IL-7 (pg/mL)	109	2.8	(2, 5.2)	39	2.4	(1.8, 4.5)	70	3.2	(2.2, 6.1)	**0.03**
IL-8 (pg/mL)	109	1.3	(0.9, 1.9)	39	1.3	(0.8, 1.9)	70	1.3	(0.9, 2)	0.4
IL-10 (pg/mL)	109	2	(0.8, 3.7)	39	1.7	(0.6, 4.3)	70	2.3	(0.9, 3.6)	0.21
IL-17a (pg/mL)	109	4.4	(3.2, 6.3)	39	3.8	(2.1, 5.6)	70	5.1	(3.6, 6.5)	**0.01**
IFNγ (pg/mL)	109	11.9	(8.5, 15.9)	39	10.5	(7.4, 14.1)	70	12.5	(9.9, 17.7)	**0.03**
TNFα (pg/mL)	109	1.6	(1.1, 2.1)	39	1.3	(0.9, 1.9)	70	1.7	(1.3, 2.2)	**0.02**
Complement 3 (mg/dL)	131	136.1	(120.1, 154.1)	45	143	(122, 162)	86	129	(119, 151)	**0.05**
Complement 4 (mg/dL)	131	28	(23.8, 32.7)	45	29.3	(22.4, 36.2)	86	27.5	(23.9, 31.4)	0.19
B2-microglobulin (mg/L)	131	1.3	(1.2, 1.4)	45	1.3	(1.2, 1.4)	86	1.3	(1.1, 1.4)	0.25
Adiponectin (mg/L)	126	9.5	(6.1, 13.7)	44	5.8	(4.5, 10.1)	82	10.9	(8.3, 16)	**<0.001**
Leptin (µg/L)	116	5.5	(3.3, 8.6)	37	6.1	(3.5, 8.8)	79	5.5	(3.2, 8.7)	0.49
Lifestyle behaviours										
Sedentary Time (min/day)	130	793	(63)	45	808	(763, 854)	85	785	(55)	0.06
Physical Activity (ENMO, mG/5s)	130	31.5	(27, 35.9)	45	30	(24.5, 36.9)	85	32	(28, 36)	0.11
Sleep Duration (min/day)	130	382	(356, 413)	45	373	(346, 403)	85	387	(364, 417)	0.14
Energy intake (24 h recall questionnaire, kcal/day)	131	1911	(477)	45	2026	(1663, 2296)	86	1798	(1556, 2096)	**0.01**
Energy intake (*ad libitum*, kcal)	119	794	(652, 1086)	44	1134.5	(425.9)	75	750.2	(254.2)	**<0.001**
Carbohydrate intake (% of Daily Energy Intake)	131	42.6	(7.3)	45	39.9	(36.1, 45.7)	86	43.8	(39.1, 47.6)	0.13
Fat Intake (% of daily energy intake)	131	40.2	(6.8)	45	40	(8)	86	40.3	(6.1)	**0**.78
Protein Intake (% of daily energy intake)	131	16.6	(14.7, 18.7)	45	17.9	(3)	86	15.9	(14, 17.4)	**<0.001**
MED score	130	24	(4.9)	45	24	(20, 26)	85	24.3	(5.2)	0.4
DASH score	126	24	(21, 28)	42	21.5	(19, 25)	84	25	(23, 29)	**<0.001**
DII score	131	-0.2	(1.5)	45	-0.7	(-1.3, 0.6)	86	-0.1	(1.6)	0.36

Table 1. Characteristics of the study subjects. Continuous variables are presented as means (standard deviation) when normally distributed, or medians (interquartile range) when not. Categorical variables are presented as numbers (percentage). No correction of outliers or transformations were performed for the descriptive data. P-values for comparisons between men and women were calculated using the independent sample Student t-test and Welch test, and the Mann-Whitney U test, for continuous variables (for normally and non-normally distributed, respectively), and the Chi-square test for categorical variables. ALP: alkaline phosphatase, ALT: alanine aminotransferase, BAT: brown adipose tissue, BMI: body mass index, DASH: dietary approach to stop hypertension, DII: dietary inflammatory index, ENMO: Euclidean norm minus one, FMI: fat mass index, GGT: gamma-glutamyl transferase, HDL-C: high-density lipoprotein-cholesterol, HOMA-IR: homeostatic model assessment of insulin resistance, HOMA-β: homeostatic model assessment of β-cell function, HU: Hounsfield units, IFNγ: interferon-gamma, LDL-C: low-density lipoprotein-cholesterol, IL: interleukins, LMI: Lean mass index, MED: Mediterranean dietary pattern, SUV: standardized uptake value, TNFα: tumor necrosis factor alpha, VAT: visceral adipose tissue.

	BAT volume					BAT SUV_{peak}					BAT mean radiodensity				
	B	**SE**	**β**	**Adj. R^2**	**P**	**B**	**SE**	**β**	**Adj. R^2**	**P**	**B**	**SE**	**β**	**Adj. R^2**	**P**
	MEN (n=45)					**MEN (n=45)**					**MEN (n=31)**				
Glucose (mg/dL)	0.009	0.017	0.081	-0.016	0.59	0.079	0.151	0.079	-0.017	0.60	-0.345	0.139	-0.418	0.146	**0.02**
Insulin (uIU/mL)	0.017	0.013	0.194	0.015	0.20	0.055	0.119	0.071	-0.018	0.64	-0.409	0.101	-0.600	0.337	**<0.001**
HOMA-IR	0.004	0.003	0.177	0.009	0.24	0.011	0.030	0.058	-0.020	0.71	-0.107	0.025	-0.622	0.366	**<0.001**
HOMA-β	0.218	0.134	0.240	0.036	0.11	0.600	1.254	0.073	-0.018	0.63	-3.499	1.191	-0.479	0.097	**0.006**
Total cholesterol (mg/dL)	0.118	0.068	0.254	0.043	0.09	0.485	0.639	0.115	-0.010	0.45	-0.296	0.666	-0.082	-0.027	0.66
LDL-C (mg/dL)	0.086	0.055	0.232	0.032	0.12	0.301	0.512	0.089	-0.015	0.56	-0.621	0.544	-0.207	-0.01	0.26
HDL-C (mg/dL)	0.028	0.017	0.247	0.039	0.10	0.193	0.153	0.189	0.013	0.21	0.394	0.133	0.482	0.206	**0.006**
Total cholesterol/HDL-C	0.001	0.002	0.083	-0.016	0.59	-0.002	0.018	-0.018	-0.023	0.91	-0.039	0.016	-0.410	-0.140	**0.022**
LDL-C/HDL-C	0.001	0.002	0.066	-0.019	0.66	-0.004	0.015	-0.040	-0.022	0.79	-0.034	0.013	-0.435	0.161	**0.015**
Triacylglycerols	0.002	0.003	0.143	-0.002	0.35	0.021	0.024	0.132	-0.005	0.39	-0.010	0.026	-0.068	-0.030	0.72
Homocysteine (µmol/L)	0.018	0.007	0.383	0.127	**0.009**	0.109	0.062	0.258	0.045	0.09	0.049	0.062	0.145	-0.013	0.44
Systolic Blood Pressure[a] (mmHg)	0.022	0.025	0.139	-0.004	0.37	0.181	0.224	0.124	-0.008	0.42	-0.343	0.236	-0.265	0.037	0.16
Diastolic Blood Pressure[a] (mmHg)	0.018	0.020	0.137	-0.004	0.37	-0.047	0.182	-0.040	-0.022	0.80	-0.270	0.167	-0.293	-0.053	0.12
CMR score	0.002	0.002	0.171	0.006	0.27	0.009	0.020	0.070	-0.019	0.65	-0.064	0.016	-0.596	0.332	**0.001**
ALT[a]	0.004	0.002	0.270	0.051	0.07	0.020	0.022	0.142	-0.003	0.35	-0.059	0.023	-0.425	0.153	**0.02**
GGT[a]	0.005	0.002	0.381	0.125	**0.01**	0.029	0.017	0.249	0.040	0.10	-0.029	0.020	-0.257	0.034	0.16
ALP (U/L)	0.088	0.036	0.346	0.099	**0.02**	0.591	0.340	0.256	0.044	0.09	-0.128	0.376	-0.063	-0.030	0.74
FLI	0.005	0.002	0.348	0.101	**0.02**	0.018	0.018	0.152	0	0.32	-0.069	0.016	-0.618	0.360	**<0.001**
	WOMEN (n=86)					**WOMEN (n=86)**					**WOMEN (n=66)**				
Glucose (mg/dL)	0.014	0.012	0.123	0.003	0.20	0.031	0.074	0.045	-0.010	0.68	0.035	0.074	0.059	-0.012	0.64
Insulin (uIU/mL)	0.004	0.008	0.058	-0.009	0.60	0.023	0.051	0.048	-0.010	0.66	-0.065	0.045	-0.178	0.016	0.15
HOMA-IR	0.001	0.002	0.061	-0.008	0.57	0.005	0.013	0.043	-0.010	0.69	-0.015	0.011	-0.159	0.010	0.20
HOMA-β	0.018	0.095	0.021	-0.011	0.85	0.294	0.578	0.055	-0.009	0.61	-0.922	0.502	-0.224	0.035	0.07
Total cholesterol (mg/dL)	-0.09	0.091	-0.159	0.014	0.14	-0.543	0.371	-0.158	0.013	0.15	0.403	0.359	0.139	0.004	0.27
LDL-C (mg/dL)	-0.07	0.049	-0.153	0.012	0.16	-0.387	0.303	-0.138	0.007	0.20	0.244	0.265	0.114	-0.002	0.36
HDL-C (mg/dL)	-0.009	0.021	-0.047	-0.010	0.67	-0.056	0.129	-0.047	-0.010	0.66	0.210	0.124	0.207	0.028	0.10
Total cholesterol/HDL-C	-0.002	0.001	-0.148	0.010	0.17	-0.009	0.007	-0.132	0.006	0.22	-0.005	0.006	-0.107	-0.004	0.39
LDL-C/HDL-C	-0.001	0.001	-0.136	0.007	0.21	-0.007	0.007	-0.116	0.002	0.29	-0.003	0.006	-0.073	-0.010	0.56
Triacylglycerols	-0.002	0.002	-0.149	0.010	0.17	-0.012	0.011	-0.120	0.003	0.27	-0.005	0.011	-0.059	-0.471	0.64
Homocysteine (µmol/L)	-0.005	0.005	-0.102	-0.001	0.35	-0.013	0.031	-0.045	-0.010	0.68	0.041	0.030	0.166	0.012	0.18
Systolic blood pressure[a] (mmHg)	-0.002	0.190	-0.012	-0.012	0.92	0.051	0.117	0.048	-0.010	0.66	0.041	0.112	0.047	-0.014	0.71
Diastolic blood pressure[a] (mmHg)	0.002	0.013	0.015	-0.012	0.89	0.026	0.080	0.036	-0.011	0.74	-0.009	0.068	-0.017	-0.016	0.89
CMR score	0.001	0.002	0.065	-0.008	0.56	0	0.013	-0.004	-0.012	0.97	-0.012	0.010	-0.151	0.007	0.24
ALT[a]	0	0.002	0.005	-0.012	0.96	0.001	0.010	0.011	-0.012	0.92	-0.002	0.009	-0.025	-0.015	0.84
GGT[a]	-0.001	0.002	-0.080	-0.005	0.46	-0.016	0.010	-0.169	0.017	0.12	-0.004	0.009	-0.054	-0.013	0.67
ALP (U/L)	-0.022	0.036	-0.068	-0.007	0.53	-0.403	0.213	-0.202	0.029	0.06	-0.445	0.207	-0.260	0.053	**0.03**
FLI	0	0.002	0.010	-0.012	0.93	-0.017	0.011	-0.162	0.014	0.14	-0.022	0.009	-0.296	0.073	**0.02**

Table 2. Associations shown by BAT volume, SUV_{peak} and mean radiodensity with cardiometabolic risk (CMR) markers in young men and women. Linear regression analyses were performed. The non-standardized regression coefficient (B), standard error (SE), standardized regression coefficient (β), and adjusted R squared (Adj. R^2) are provided. A subtle variation of winsorizing was performed on the extreme outliers of outcome results, and some variables were transformed using Box Cox transformations (see Appendix B). Transformed variables are unitless. Similar results were observed with outliers corrected and not corrected, except for the association of BAT SUV_{peak} with the homocysteine concentration, and of BAT mean radiodensity with HOMA-B (which were non-significant; $P>0.05$), and of BAT SUV_{peak} with ALT levels (which were significant; $P<0.05$) when outliers were corrected for the men. ALP: alkaline phosphatase, ALT: alanine aminotransferase, BAT: brown adipose tissue, GGT: gamma-glutamyl transferase, HDL-C: high-density lipoprotein-cholesterol, HOMA-IR: homeostatic model assessment of insulin resistance, HOMA-β: homeostatic model of β-cell function, LDL-C: low-density lipoprotein-cholesterol, SUV: standardized uptake value. Outcomes with the superscript [a] had 1 missing subject.

	BAT volume					BAT SUV_{peak}					BAT mean radiodensity				
	B	**SE**	**β**	**Adj. R^2**	**P**	**B**	**SE**	**β**	**Adj. R^2**	**P**	**B**	**SE**	**β**	**Adj. R^2**	**P**
	MEN (n=45)					**MEN (n=45)**					**MEN (n=31)**				
C-reactive protein	0.003	0.002	0.216	0.024	0.15	0.025	0.018	0.203	0.019	0.18	-0.029	0.019	-0.280	0.046	0.13
IL-2[a] (pg/mL)	-0.004	0.004	-0.201	0.015	0.22	-0.053	0.029	-0.284	0.056	0.08	-0.027	0.030	-0.184	-0.008	0.38
IL-4[a]	-0.002	0.003	-0.126	-0.011	0.44	-0.019	0.023	-0.136	-0.008	0.41	-0.031	0.026	-0.238	0.016	0.25
IL-6[a] (pg/mL)	-0.003	0.005	-0.091	-0.018	0.58	-0.019	0.038	-0.080	-0.020	0.63	-0.035	0.040	-0.177	-0.011	0.40
IL-7[a]	-0.001	0.003	-0.034	-0.026	0.83	-0.010	0.022	-0.075	-0.021	0.65	-0.026	0.023	-0.228	0.011	0.27
IL-8[a]	-0.003	0.003	-0.183	0.007	0.27	-0.029	0.024	-0.198	0.013	0.23	-0.033	0.026	-0.260	0.027	0.21
IL-10[a] (pg/mL)	-0.006	0.006	-0.166	0.001	0.31	-0.041	0.048	-0.139	-0.007	0.40	0.001	0.053	0.003	-0.043	0.99
IL-17a[a] (pg/mL)	-0.005	0.005	-0.153	-0.003	0.35	-0.087	0.044	-0.307	0.070	0.06	-0.039	0.055	-0.146	-0.021	0.49
IFNγ[a] (pg/mL)	-0.016	0.013	-0.187	0.009	0.25	-0.118	0.113	-0.170	0.003	0.30	0.031	0.120	0.054	-0.040	0.80
TNFα[a] (pg/mL)	-0.003	0.002	-0.226	0.026	0.17	-0.016	0.015	-0.167	0.002	0.31	0.006	0.014	0.085	-0.036	0.69
Complement 3 (mg/dL)	0.167	0.053	0.434	0.170	**0.003**	1.159	0.506	0.330	0.088	**0.03**	-1.145	0.509	-0.385	0.119	**0.03**
Complement 4 (mg/dL)	0.021	0.022	0.146	-0.001	0.34	0.258	0.197	0.195	0.016	0.20	0.029	0.208	0.026	-0.034	0.89
B2-microglobulin (mg/L)	0	0	0.041	-0.022	0.79	0.003	0.004	0.106	-0.012	0.49	0.006	0.005	0.243	0.026	0.19
Adiponectin[b] (mg/L)	0.005	0.012	0.068	-0.019	0.66	0.096	0.111	0.132	-0.006	0.39	0.285	0.108	0.445	0.169	**0.01**
Leptin[c] (µg/L)	0.006	0.011	0.101	-0.018	0.55	0.094	0.098	0.160	-0.002	0.34	-0.019	0.112	-0.036	-0.042	0.87
	WOMEN (n=86)					**WOMEN (n=86)**					**WOMEN (n=66)**				
C-reactive protein	0.005	0.002	0.230	0.041	**0.03**	0.016	0.013	0.135	0.006	0.22	-0.024	0.012	-0.237	0.041	**0.05**
IL-2[a] (pg/mL)	0.002	0.003	0.082	-0.008	0.50	0.020	0.018	0.137	0.004	0.26	0.017	0.019	0.121	-0.004	0.38
IL-4[a]	0.002	0.002	0.093	-0.005	0.43	0.012	0.013	0.117	-0.001	0.34	0.009	0.013	0.092	-0.011	0.51
IL-6[a] (pg/mL)	0.001	0.004	0.024	-0.014	0.84	0.013	0.022	0.068	-0.010	0.58	-0.012	0.024	-0.069	-0.014	0.62
IL-7[a]	0.001	0.002	0.080	-0.008	0.51	0.024	0.012	0.225	0.037	0.06	0.022	0.013	0.225	0.032	0.10
IL-8[a]	0	0.002	0.010	-0.015	0.94	0.008	0.013	0.077	-0.009	0.53	0.002	0.014	0.020	-0.019	0.88
IL-10[a] (pg/mL)	0.004	0.006	0.082	-0.008	0.50	0.046	0.035	0.156	0.010	0.20	0.096	0.037	0.334	0.095	**0.01**
IL-17a[a] (pg/mL)	0.001	0.004	0.018	-0.014	0.88	0.008	0.027	0.037	-0.013	0.76	0.025	0.030	0.117	-0.005	0.40
IFNγ[a] (pg/mL)	0.007	0.011	0.078	-0.009	0.52	0.033	0.071	0.056	-0.011	0.64	0.105	0.077	0.185	0.016	0.18
TNFα[a] (pg/mL)	-0.001	0.002	-0.092	-0.006	0.45	-0.006	0.011	-0.061	-0.011	0.62	0.008	0.011	0.099	-0.009	0.48
Complement 3 (mg/dL)	0.043	0.043	0.109	0	0.32	-0.062	0.266	-0.025	-0.011	0.82	-0.519	0.255	-0.246	0.046	**0.05**
Complement 4 (mg/dL)	0.023	0.016	0.154	0.012	0.16	0.090	0.099	0.098	-0.002	0.37	-0.077	0.098	-0.098	-0.006	0.43
B2-microglobulin (mg/L)	0	0	0.090	-0.004	0.41	-0.001	0.003	-0.043	-0.010	0.69	0.002	0.003	0.087	-0.008	0.49
Adiponectin[b] (mg/L)	0.023	0.015	0.170	0.017	0.13	0.070	0.090	0.086	-0.005	0.44	0.113	0.086	0.165	0.011	0.20
Leptin[c] (µg/L)	0	0.008	0.002	-0.013	0.98	-0.037	0.048	-0.088	-0.005	0.44	0.043	0.053	0.106	-0.006	0.42

Table 3. Associations shown by BAT volume, SUV_{peak} and mean radiodensity with inflammatory markers in young men and women. The sample size (B), non-standardized regression coefficient (SE). standard error (β), standardized regression coefficient and adjusted R^2 values are provided. A subtle variation of winsorizing was performed on the extreme outliers of outcome results, and some variables were transformed using Box Cox transformations (see Appendix B). Transformed variables are unitless. Similar results were observed with outliers corrected and uncorrected, except for the association of BAT volume with adiponectin levels – which was significant ($P<0.05$) - and of BAT mean radiodensity with IL-10 levels (which was non-significant; $P>0.05$) when outliers were not corrected in women. BAT: brown adipose tissue, IFNγ: interferon-gamma, IL: interleukin, SUV: standardized uptake value, TNFα: tumor necrosis factor alpha. Some specific outcomes had missing data for men: [a]6 missing subjects, [b]1 missing subjects, [c]8 missing subjects; and for women: [a]16 missing subjects, [b]4 missing subjects, [c]7 missing subjects.

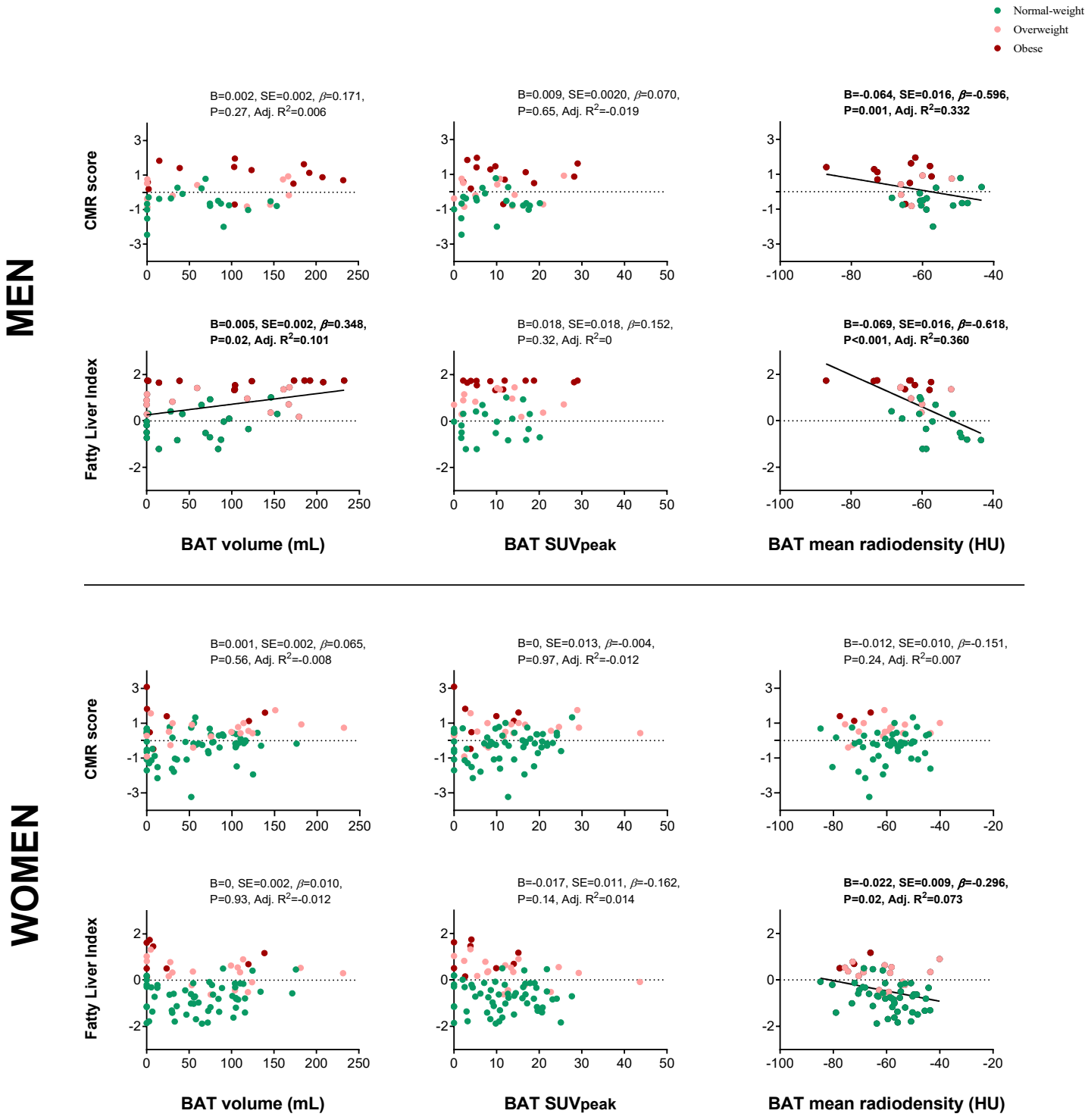

Figure 1. Scatter plots for linear regressions involving BAT volume, SUV_{peak} or mean radiodensity against the cardiometabolic risk (CMR) score and the fatty liver index, in young men and women (Table 2). B: non-standardized regression coefficient, SE: standard error, β: standardized regression coefficient and Adj. R^2: adjusted R squared are provided). The CMR score and fatty liver index were winsorized and transformed. The sample size for men was 45 (except for BAT mean radiodensity, n=31) and for women 86 (except for BAT mean radiodensity, n=66). BAT: brown adipose tissue, CMR: cardiometabolic risk, SUV: standardized uptake value.

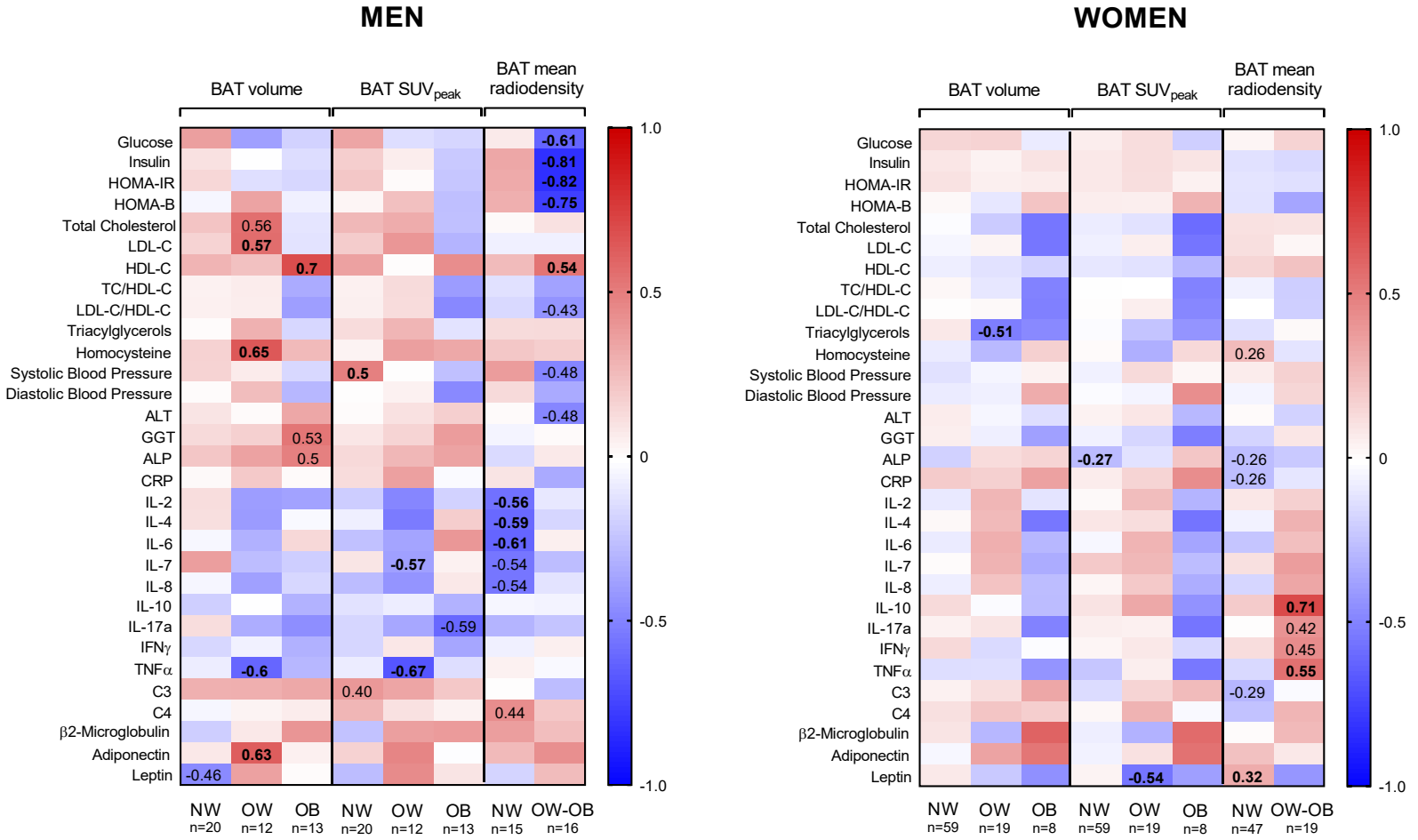

Figure 2. Associations shown by BAT volume, SUV_{peak} and mean radiodensity with cardiometabolic risk and inflammatory markers in young men and women, according to the subject body weight. The heat map shows the strength of the Pearson correlations; the darker the colour of the square, the stronger the correlation is (the dark red colour represents a Pearson coefficient of 1, and the dark blue colour represents a negative Pearson coefficient of -1). The Pearson correlation coefficient is provided for those associations with a P value of ≤0.1, and shown in bold for significant associations of P≤0.05). A subtle variation of winsorizing was performed on the extreme outliers of outcome results, and some variables were transformed using Box Cox transformations (Appendix B). ALP: alkaline phosphatase, ALT: alanine aminotransferase, BAT: brown adipose tissue, GGT: gamma-glutamyl transferase, HDL-C: high-density lipoprotein-cholesterol, HOMA-IR: homeostatic model assessment of insulin resistance, HOMA-β: homeostatic model of β-cell function, IFNγ: interferon-gamma, IL: interleukin, LDL-C: low-density lipoprotein-cholesterol, SUV: standardized uptake value, TC: total cholesterol, TNFα: tumor necrosis factor alpha. Some specific outcomes had some missing data for men: 1 missing subject for systolic and diastolic blood pressure, adiponectin, 6 for IL-2, IL-4, IL-6, IL-7, IL-8, IL-10, IL-17a, IFN, TNFα), and 8 for leptin; and for women: 1 missing for systolic and diastolic blood pressure, ALT, GGT, 3 for FLI, 4 for adiponectin, 7 for leptin, and 16 for IL-2, IL-4, IL-6, IL-7, IL-8, IL-10, IL-17a, IFN, TNFα.